J Nanopart Res (2016) 18:85
DOI 10.1007/s11051-016-3391-4

RESEARCH PAPER

# Cytotoxicity of semiconductor nanoparticles in A549 cells is attributable to their intrinsic oxidant activity

**Vicente Escamilla-Rivera · Marisela Uribe-Ramirez · Sirenia Gonzalez-Pozos · Subramaniam Velumani · Laura Arreola-Mendoza · Andrea De Vizcaya-Ruiz**

Received: 5 November 2015 / Accepted: 8 March 2016 / Published online: 23 March 2016


**Abstract** Copper indium gallium diselenide (CIGS) and cadmium sulfide (CdS) nanoparticles (NP) are next generation semiconductors used in photovoltaic cells (PV). They possess high quantum efficiency, absorption coefficient, and cheaper manufacturing costs compared to silicon. Due to their potential for an industrial development and the lack of information about the risk associated in their use, we investigated the influence of the physicochemical characteristics of CIGS (9 nm) and CdS (20 nm) in relation to the induction of cytotoxicity in human alveolar A549 cells through ROS generation and mitochondrial dysfunction. CIGS induced cytotoxicity in a dose dependent manner in lower concentrations than CdS; both NP were able to induce ROS in A549. Moreover, CIGS interact directly with mitochondria inducing depolarization that leads to the induction of apoptosis compared to CdS. Antioxidant pretreatment significantly prevented the loss of mitochondrial membrane potential and cytotoxicity, suggesting ROS generation as the main cytotoxic mechanism. These results demonstrate that semiconductor characteristics of NP are crucial for the type and intensity of the cytotoxic effects. Our work provides relevant information that may help guide the production of a safer NP-based PV technologies, and would be a valuable resource on future risk assessment for a safer use of nanotechnology in the development of clean sources of renewable energy.

**Keywords** Cu–In–Ga–$Se_2$ · CdS · Semiconductor nanoparticles · Nanotoxicology · Photovoltaics · Health effects

V. Escamilla-Rivera · M. Uribe-Ramirez · A. De Vizcaya-Ruiz (✉)
Departamento de Toxicología, Centro de Investigación y de Estudios Avanzados del IPN (CINVESTAV-IPN), P.O. Box 14-740, Av. Instituto Politécnico Nacional 2508, Col. San Pedro Zacatenco, C.P. 07360 Mexico, DF, Mexico
e-mail: avizcaya@cinvestav.mx

S. Gonzalez-Pozos
Unidad de Microscopia Electrónica (LaNSE), CINVESTAV-IPN, Mexico, DF, Mexico

S. Velumani
Departamento de Ingeniería Eléctrica, CINVESTAV-IPN, Mexico, DF, Mexico

L. Arreola-Mendoza
Departamento de Biociencias e Ingeniería, Centro Interdisciplinario de Investigaciones y Estudios sobre Medio Ambiente y Desarrollo del Instituto Politécnico Nacional (CIIEMAD-IPN), Mexico, DF, Mexico

## Introduction

Nanotechnology is an emerging discipline that has introduced new dimensions to science and technology, with the possibility of manipulating atoms and single molecules at the nanoscale level (Maynard 2007). The energy generation field is one of the most benefited

sectors from nanotechnology driving it into a more sustainable process, the use of NP has led to the development of better and safer hydrogen storages, fuel cells, and photovoltaic solar cells (PV) among others (Liu et al. 2010). There are several PV technologies in the field, such as crystalline or amorphous silica thin-film, cadmium telluride (CdTe), and cadmium sulfide (CdS) nanocrystals, polymer-based, and copper indium gallium diselenide (CIGS) thin films cells (Bagnall and Boreland 2008). CIGS and CdS NP are semiconductor nanoparticles (NP) specifically designed to improve the efficiency of PV by increasing the capture of photons and converting them into free electrons. CIGS NP in conjunction with CdS NP have recorded efficiencies (solar to electric energy conversion) up to 20.3 % (Jackson et al. 2011), and they have emerged as a cheap, efficient, and eco-friendly alternative to the traditional silicon-based solar cells (Reinhard et al. 2013). Nowadays, CIGS NP are considered as the most promising materials for PV devices (Dhere 2007). Moreover, it has also been projected that the replacing of traditional grid electricity with PV systems results in 89–98 % reductions in emissions of greenhouse gases, criteria pollutants, and heavy metals (Fthenakis 2009).

However, there is still a significant concern about the adverse effects related to NP used in PV, due to the novel properties that make them desirable which also confer more reactivity in biological systems (Nel et al. 2006). It is clear that, if the materials that compose the PV module do not degrade during their lifetime, synthesis and disposal of CIGS and CdS containing-devices would be the critical exposure stages, because of the potential release and resuspension of powders into the air, leading to a NP-enriched atmosphere that can be inhaled (Dreher 2004; Oberdörster 2010).

Generation of reactive oxygen species (ROS) by NP is considered so far the major contributor to their toxicity. Semiconductor NP can produce ROS by several mechanisms (1) acting as catalyzers by transferring electrons from reduced molecules to oxygen, (2) by total or partial dissolution of its components, i.e., transition metals that can participate in Fenton like reaction, and (3) upon cell contact by the physical interaction of NP with substructures involved in the catalysis of biological redox reactions like mitochondria and phagolysosomes. ROS react with a wide range of biological targets. It is well known that low concentrations of ROS are necessary to carry out signaling steps of vital process for the cell. However, under conditions when the formation of ROS is enhanced, they can exert its deleterious effects via macromolecule oxidation, gene transcription. and impairment of organelles such as mitochondrial function and compromising the viability of cells (Valko et al. 2007). Upon the impact in cellular homeostasis, cells can either repair the damage or activate pathways that lead to apoptosis (Martindale and Holbrook 2002; Ott et al. 2007) or other forms of cell death.

There are few reports that have addressed the toxic potential of the precursors of CIGS PV; nonetheless, none of them have been focused on the safety of CIGS or CdS NP per se (Eisenberg et al. 2013; Fthenakis and Moskowitz 2000). To the best of our knowledge, there are no reports concerning to the toxicity of CIGS NP; therefore we attempted to investigate the influence of the physicochemical characteristics and probable oxidant properties of CIGS and CdS in relation to the induction of cytotoxicity in A549 (human lung carcinoma) cells through mitochondrial dysfunction, ROS intracellular generation, and cell death. CIGS and CdS NP were characterized for size, agglomeration state, surface charge, and cellular uptake using dynamic light scattering (DLS) and electron microscopy (SEM and TEM). This approach allowed to investigate the potential toxicity for CIGS and CdS NP, providing relevant information for the production of safer NP-based PV technologies and a valuable resource for future risk assessment studies and safer use of nanotechnology.

## Materials and methods

### Chemicals and nanopowders

Dithiothreitol (DTT) 5,5′-dithiobis(2) dinitrobenzoic acid (DTNB), 3-(4,5-dimethylthiazol-2-yl)-2,5-diphenyl tetrazolium bromide MTT, Tetramethylrhodamine ethyl ester perchlorate (TMRE), Carbonyl cyanide 4-(trifluoromethoxy)phenylhydrazone (FCCP) IGEPAL, HAM's culture media,and (±)-6-Hydroxy-2,5,7,8-tetramethylchroman-2-carboxylic acid (Trolox) were obtained from Sigma Aldrich. 2, 7-dichlorofluorescein diacetate DCFH-DA, MitoTracker Green and Dead Cell Apoptosis Kit were obtained from Molecular Probes. All other chemicals used were obtained from commercial sources and were of the

highest grade available. CIGS and CdS NP were synthesized by Dr. Velumani Subramaniam (Department of Electrical Engineering, Cinvestav) thorough mechanical alloying from high purity precursors mixed in a planetary ball mill. CIGS and CdS NP obtained by this method are highly pure with the characteristic tetragonal chalcopyrite crystal structure for CIGS and a typical hexagonal crystal structure for CdS with no evidence of phase transition from hexagonal to cubic structure. Electrical properties and chemical characteristics have been reported previously in Reyes and Velumani (2012) and Vidhya (2010).

### Redox activity determined by dithiothreitol (DTT) assay

The redox activity of the NP was assessed by its ability to catalyze the transfer of electrons from DTT to oxygen as described by Cho (2005); briefly, three tubes containing 0.5 M PBS, pH 7.4, 1 mM DTT, and NP suspensions (40 μg/mL) in double deionized water were incubated at 37 °C in the dark. At pre-defined times, ranging from 0 to 45 min, the DTT oxidation was quenched by adding 1000 μL of trichloroacetic acid 10 %, and a portion of the mixture was dissolved with a Tris buffer at pH 8.9, 20 mM EDTA and 10 mM DTNB solution. The remaining DTT was reacted with DTNB, generating 5-mercapto-2-nitrobenzoic acid whose concentration was determined colorimetrically at 412 nm in a SpectraMax Plus microplate Reader (Molecular Devices). The redox activity is expressed as the rate of DTT consumption (pmol) per minute per microgram of sample minus the activity observed in the absence of NP.

### NP suspension and characterization

Nanoparticle stock solutions (1 mg/mL) were prepared by dispersing the NP powder in double deionized water by probe sonication for 2 min. To ensure the maximum dispersion, the different types of NP were prepared in suspensions with 2 mg/mL of bovine serum albumin (BSA) and equilibrated for 1 h at room temperature. The NP suspensions were sonicated for 15 s prior to the addition to culture media and diluted to reach the desired concentrations (Xia et al. 2008). In order to verify the stability of the NP dispersion we compared NP suspensions, before and after the addition of BSA analyzing the hydrodynamic diameter and zeta potential by dynamic light scattering (DLS) using the Zetasizer Nano ZS90 size analyzer (Malvern Instruments Ltd) and comparing the overall agglomeration with scanning electron microscopy (SEM), conducted in a HRSEM- AURIGA (ZEISS) electron microscope.

### Cell culture and exposure to NP

A549 human lung carcinoma cells were obtained from ATCC (CRM-CCL-185). Cells were subcultured in HAM's culture media supplemented with pyruvate 0.05 mg/mL, 2 mM L-glutamine, penicillin/streptomycin (50 IU/mL and 50 g/mL, respectively), and 10 % (v/v) FBS. They were maintained at 37 °C in a 5 % $CO_2$/air incubator and passed at 80 % confluence. For all the experiments, cells were seeded in 24 well-plates at $5 \times 10^4$ cells/cm$^2$ for 24 h prior exposure to NP; after that, cells were washed with PBS and changed to exposure media consisting in HAM'S supplemented with 0.5 % FBS and NP suspensions in concentrations of 6.25, 12.5, 25, 50, 100, and 200 μg/mL, in time lapses of 6, 16, 24, 48, and 72 h. For Trolox experiments, cells were pretreated 30 min before NP exposure with trolox 100 μM dissolved in PBS.

### NP cell uptake

A549 cells were exposed to 25 μg/mL of CIGS and CdS NP for 24 h, then cells were washed two times with cacodylate buffer and fixed with 2.5 % of glutaraldehyde at 4 °C; after fixation, the cells were collected and stained with osmium tetroxide. Then they were dehydrated in acetone series (50–100 %) and embedded in epoxy medium EPON 812 (Electronic Microscopy Sciences). Ultrathin sections of 50 nm were obtained with an ultramicrotome (Leica EM UC7) and stained with uranyl acetate followed by lead citrate and were examined using a JEM 1400 (JEOL) electron microscope at 80 keV.

### MTT viability assay

Cytotoxicity was assessed using the MTT assay (Mosmann 1983). Mitochondrial dehydrogenases of viable cells reduce MTT to water-insoluble formazan crystals, which are solubilized by acidic isopropanol. After exposure to the NP suspensions, 100 μL of a

5 mg/mL MTT solution was added to each well, and incubated for 4 h at 37 °C; then the medium was discarded and replaced by 1000 μL of acidic isopropanol with 1 % (v/v) of IGEPAL and mixed thoroughly to dissolve the formazan crystals. To avoid potential problems due to the possible presence of residual NP that could interfere with the assay, the supernatants were centrifuged at 14,000×*g* for 15 min before absorbance reading at 570 nm with a SpectraMax Plus microplate Reader (Molecular Devices). Cell cytotoxicity was determined as a percentage of the negative control (unexposed cells).

### Intracellular ROS generation

The level of intracellular ROS was measured using DCFH-DA a molecule that freely enters into the cells and can be oxidized by $H_2O_2$ to form the fluorescent compound dichlorofluorescein (DCF). After NP exposure DCFH-DA 20 μM was added to the wells and incubated for 4 h at 37 °C, then the cells were rinsed with PBS and DCF fluorescence intensity was measured in a multiwell plate reader Infinite 200 (Tecan Group Ltd.), with an excitation emission wavelength 480/515 nm.

### Mitochondrial membrane potential (Δψm)

Changes in Δψm induced by NP exposure was evaluated using TMRE and Mitotracker Green® as reported elsewhere (Kamp et al. 2002). TMRE is a cationic fluorescent dye that stains selectively the mitochondria and is not retained in cells upon collapse of the Δψm. Mitotracker Green labels the mitochondria because it binds mitochondrial lipids and is not influenced by the Δψm. After NP exposure, the cells were exposed to either 500 nM TMRE or 1 μM Mitotracker green for 1 h at 37 °C. In addition, 20 μM of the protonophore FCCP, was added to separate a group of comparably treated cells for 1 h before adding fluorochromes to induce a maximal mitochondrial depolarization as positive control. Changes in dye fluorescence at 25 °C were analyzed in a multiwell-plate reader Infinite 200 (Tecan Group Ltd.), using an excitation/emission wavelength of 535 nm/575 nm for TMRE and 490 nm/516 nm for Mitotracker Green. The Δψm was compared qualitatively based upon the percentage difference in the ratio of TMRE and Mitotracker Green fluorescence of untreated cells corrected for the background fluorescence in FCCP-treated control cells.

### Apoptosis

To determine the potential induction of apoptosis from NP exposure, we used the Alexa Fluor 488 Annexin V/Dead Cell Apoptosis Kit® (Invitrogen) which detects the externalization of phosphatidylserine in apoptotic cells using annexin V conjugate. The percentage of cells that bind annexin V were obtained by flow cytometry following the manufacturer's instructions, briefly, after NP exposure cells were trypsinized, washed with PBS, and incubated with the fluorescent probe and then the cells were analyzed in a FACSCalibur flow cytometer (Becton, Dickinson and Company).

### Statistical analysis

Experiments were carried out in triplicate in three independent experiments and results were expressed as mean ± S.D. Statistical analysis was performed using the SigmaStat Software 10.0 (Systat Software Inc.). Difference between the groups was analyzed by one-way ANOVA for normally distributed data and Kruskal–Wallis for non-normally distributed data. Differences with $p < 0.05$ (*) or $p < 0.01$ (**) were considered statistically significant.

## Results

### Physicochemical characterization of NP

SEM micrographs are shown in Fig. 1, big size agglomerates of CIGS and CdS NP in ultrapure water suspensions are evident (left panel); addition of BSA to the initial NP suspensions led to their overall deagglomeration and stability (right panel). Table 1 shows the physicochemical properties of NP dispersed in water compared to BSA-stabilized suspension in culture media. Hydrodynamic diameter values showed agglomeration and polydisperse populations for CIGS (461 nm PdI 0.475) and CdS NP (628 nm PdI 0.554) in water. Addition of BSA and suspension in Ham's F-12 culture media slightly decreased the size of agglomerates; these results are consistent with zeta potential values which exhibit a poor electrostatic repulsion in water (−25.8 and −22.1 mV) and Ham's

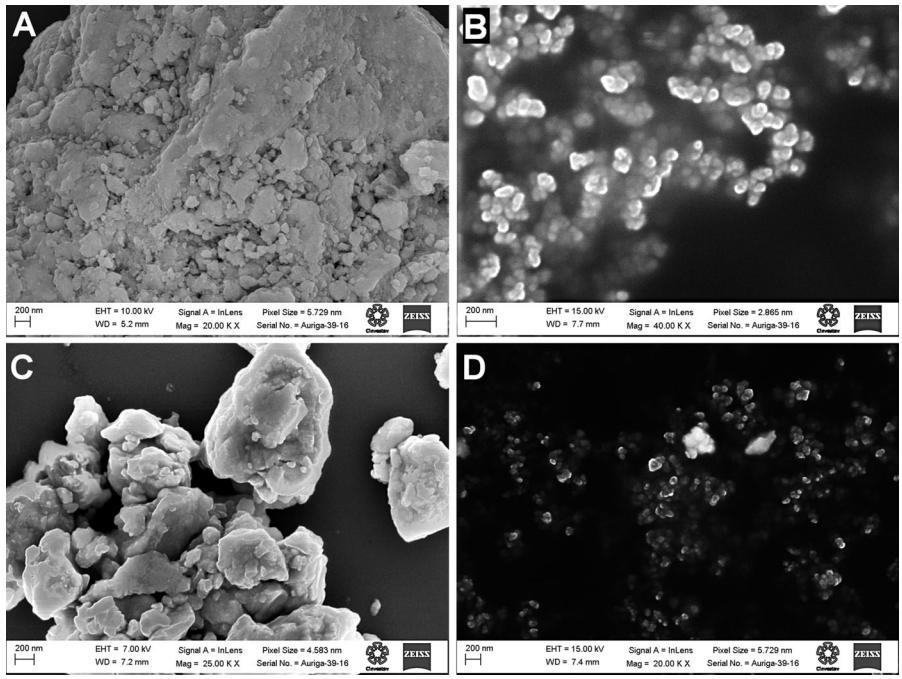


**Fig. 1** Characterization of NP dispersed in water and after BSA treatment. SEM micrographs of NP dispersed in water CIGS (**a**), CdS (**c**). BSA treatment led to a reduction in the size and number of agglomerates of CIGS (**b**) and CdS (**d**)

**Table 1** Physicochemical characterization of NP

| | Primary size (nm)[a] | Hydrodynamic diameter (nm)[b] | | | | Zeta potential (mV)[c] | |
|---|---|---|---|---|---|---|---|
| | | $H_2O$ | | HAM's F-12 | | $H_2O$ | HAM's F-12 |
| | | Z-average | PdI | Z-average | PdI | | |
| CIGS | 9 | 461 | 0.475 | 357 | 0.534 | −25.8 | −14.7 |
| CdS | 20 | 628 | 0.554 | 533 | 0.426 | −22.1 | −17.2 |

[a] Primary sizes were calculated from XRD patterns in (Reyes and Velumani 2012; Vidhya 2010)

[b] Hydrodynamic diameter determined by dynamic light scattering

[c] Zeta potential of the nanoparticles was measured by Laser Doppler Anemometry in a Zetasizer Nano ZS90 at 25 µg/mL and 25 °C

F-12 (−14.7 and −17.2 mV), for CIGS and CdS, respectively. Despite the fact that the dispersion process could not significantly decrease the size of agglomerates, BSA offers an external steric repulsion to face the imminent agglomeration of colloids that is known to occur in high ionic strength environments like Ham's F-12 according to DLVO theory (Jiang et al. 2008).

## Cellular uptake and intracellular localization of CIGS and CdS NP

The localization of CIGS and CdS NP as well as morphological changes in A549 cells was determined by TEM microscopy. Untreated cells showed the distinguishable features of A549 cells, like typical cuboidal epithelial shape, presence of lamellar bodies, an extensive cytoplasm, healthy mitochondria, and well-defined endoplasmic reticulum and Golgi complex (Fig. 2a–c). After 24 h of exposure to 25 µg/mL of CIGS NP (Fig. 2d–f), these were localized as small agglomerates both contained in membrane-bound vesicles and free NP scattered in the cytoplasm; evident mitochondrial disruption induced by CIGS can be observed due to elongation and loss of cristae of this organelle, also dilation of smooth endoplasmic reticulum is observed. On the other hand, CdS NP (Fig. 2g–i) were found only present inside vesicles

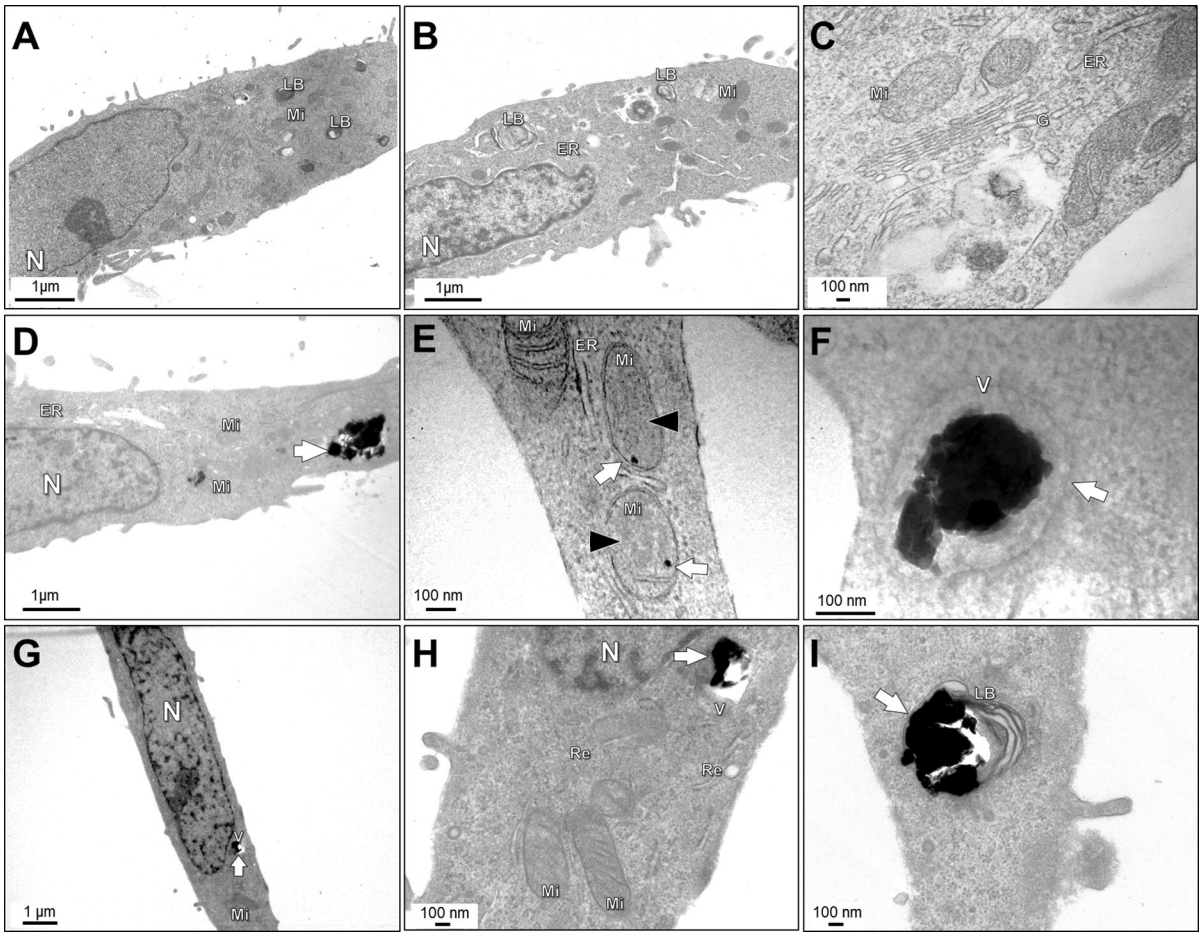


**Fig. 2** Uptake of CIGS and CdS NP by A549. Representative TEM micrographs of A549. **a–c** unexposed cells, **d–f** A549 exposed to 25 µg/mL of CIGS and **g–i** exposed to 25 µg/mL of CdS NP. *N* nucleus, *Mi* mitochondria, *LB* lamellar bodies, *V* vesicles, *G* golgi complex, *ER* endoplasmic reticulum. The *white arrows* indicate where NP are internalized. *Dark arrowheads* show loss of cristae in mitochondria of exposed cells

mainly contained in multilamellar bodies. There was no observable NP or effects in cell nucleus.

## Cytotoxicity

After the exposure at increasing concentrations ranging from 0 to 200 µg/mL of CIGS and CdS NP, cytotoxicity was evaluated using the MTT reduction method in A549 cells. CIGS NP were able to elicit high toxicity even in shorter time periods in a dose-response fashion with cell death ranging from 32 to 66 % versus control (Fig. 3a). On the other hand, CdS NP induced less toxicity compared to CIGS (Fig. 3b), and it was significantly evident from 16 h post-exposure at 100 µg/mL with a 12 % versus control (Fig. 3b).

## Nanoparticle redox activity

Considering that the generation of ROS is the main mechanism by which NP can exert their toxic effects when in contact with living organisms, we decided to initially evaluate the ability of PV NP to generate ROS spontaneously in a reductive *acellular* microenvironment. The DTT oxidation assay has been used previously to demonstrate the redox activity of various organic compounds such as quinones (Kumagai et al. 2002), particulate matter (De Vizcaya-Ruiz et al. 2006), and more recently NP (Frick et al. 2011;

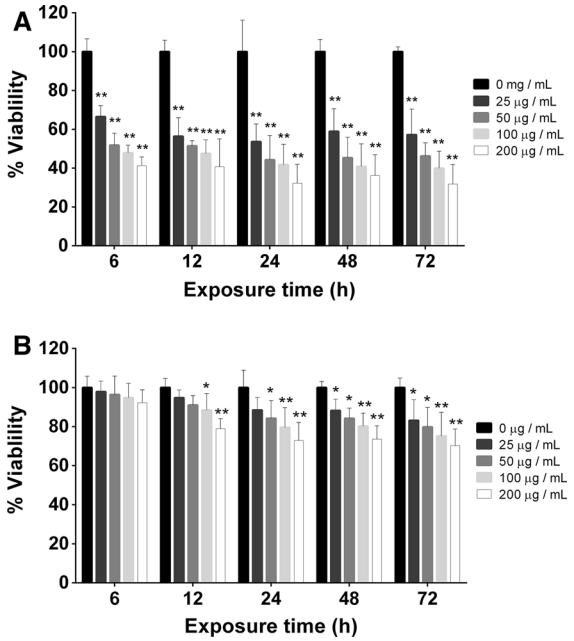


**Fig. 3** Cytotoxicity of A549 cells exposed to CIGS and CdS. **a** CIGS NP were able to elicit high toxicity even in short time periods in a dose-response manner. **b** On the other hand, CdS NP induced less toxicity, and it was only noteworthy at 16 h with 100 µg/mL. *Each point* represents the mean ± SD of three independent experiments. $*p < 0.05$ versus control, $**p < 0.001$ versus control. ANOVA, Tukey

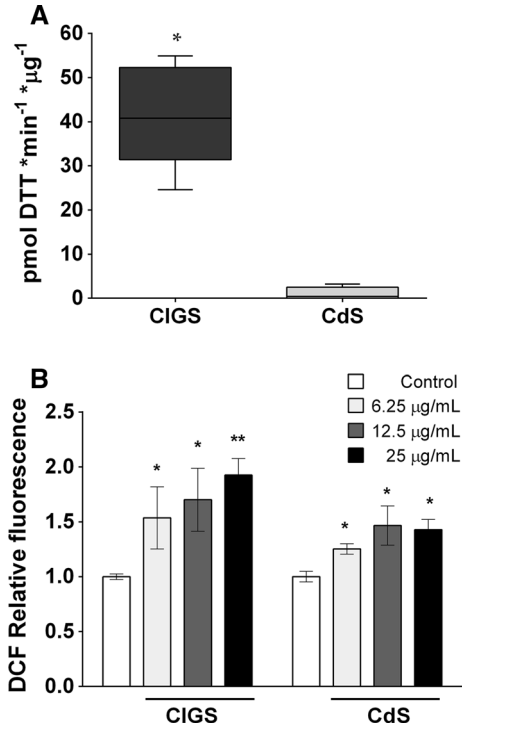


**Fig. 4** Acellular and cellular oxidant activity of NP. **a** DTT consumption, *each box* represents 25–75 % with max and min. *Asterisks* denotes difference between the groups $p < 0.05$. Mann–Whitney test. **b** DCF fluorescence in A549 cells. *Each bar* represents the mean ± SD of three independent experiments. $*p < 0.05$ versus control, $**p < 0.001$ versus control. ANOVA, Tukey

Sauvain et al. 2008). Using this technique, it is possible to detect whether any material has intrinsic oxidant properties due to its ability to transfer electrons from DTT to oxygen to form $O_2^-$ (Cho 2005). Among the two NP tested, CIGS NP had the greatest oxidant activity with a rate consumption of 41.21 pmol DTT $\times$ $\mu g^{-1} \times min^{-1}$ compared to 1.2 pmol DTT $\times$ $\mu g^{-1} \times min^{-1}$ for CdS (Fig. 4a).

In addition, to clarify if the intrinsic oxidant activity of NP could lead to an increase of intracellular ROS levels, we used the DCFH-DA assay. Exposure to NP showed that CIGS at 25 µg/mL induced a statistically significant increase in the oxidation of the DCFH molecule in a concentration-dependent manner from 6 h of exposure (Fig. 4b), with a maximum of 1.92-fold versus control. On the other hand, CdS NP increased statistically DCF fluorescence 1.5-fold, although no concentration dependence was evident. It is important to note that a constant increase in DCF fluorescence was observed at 6.25, 12.5, and 25 µg/mL with the exposure to CIGS, while CdS maintained a constant level of ROS generation of 1.2–1.5-fold.

## Mitochondrial membrane potential (Δψm)

Increased intracellular ROS levels can affect several biomolecules and organelles, including mitochondria, leading to cellular dysfunction and potentially exacerbating ROS production. We therefore analyzed whether PV NP was directly affecting mitochondria through the measurement of the loss in Δψm, using a fluorometric technique which measures the ratio between the TMRE and Mitotracker Green® fluorescence. After 24 h of exposure to 25 µg/mL, both, CIGS and CdS NP induced depolarization of the mitochondrial inner membrane (Fig. 5a), CIGS being a more potent inductor with a 40 % loss of relative Δψm compared with 28 % induced by CdS. Apparently, the CIGS and CdS deleterious effect in mitochondria varies in time from 6 h, 27 and 35 % decrease in Δψm, respectively (data not shown).

Apoptosis detection

Due to the oxidant behavior and the compromised mitochondria integrity observed from the exposure to PV NP, we decided to investigate the possible outcomes of these events evaluating the induction of apoptosis using Annexin V positive cells as an early and reliable indicator of apoptosis. After 24 h, CIGS NP induced cell death via apoptosis in 82 % of exposed cells (Fig. 5b), on the other hand 57 % of the cells exposed to CdS NP underwent apoptosis.

Antioxidant (trolox) treatment to determine ROS modulation

In order to confirm the key role of ROS in CIGS and CdS NP toward the induction of cytotoxicity, we decided to test whether an antioxidant agent could prevent the mitochondrial depolarization and cell death. Trolox, a water-soluble vitamin E analog, is a potent scavenger of ROS and is useful to maintain antioxidant capacity of cells (Forrest et al. 1994). Pretreatment with Trolox (100 μM) was able to effectively prevent the decrease in Δψm induced by CIGS and CdS at 25 μg/mL in A549 cells (Fig. 5a inset). In addition, Trolox was able to prevent the cytotoxic effects elicited by CIGS NP (Fig. 5b inset).

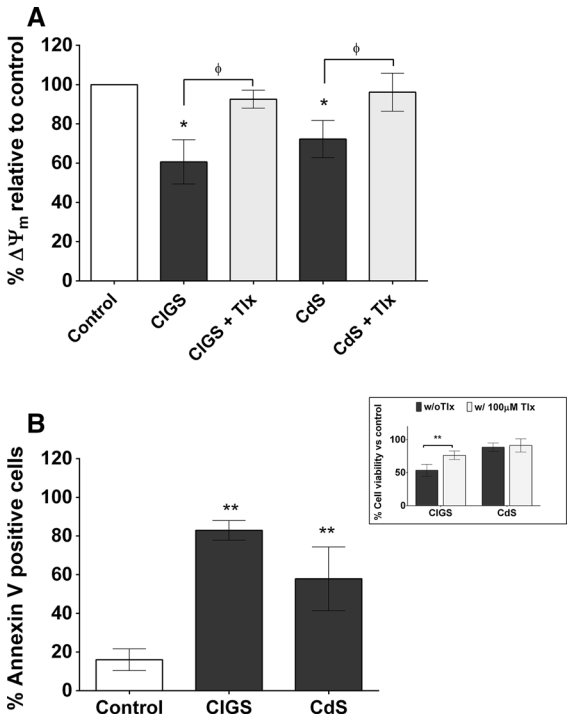


**Fig. 5** NP causes loss in Δψm and death by apoptosis mediated by ROS. **a** A549 were exposed to 25 μg/mL of CIGS and CdS, then **a** Δψm was evaluated with the ratio between TMRE/MitoTracker Green fluorescence both CIGS and CdS NP affect the mitochondria with 40 % loss of Δψm. Tlx pretreatment prevented the decrease of Δψm. **b** CIGS and CdS increase the percentage of apoptosis positive cells as measured by flow cytometry. Cell death was prevented by Tlx pretreatment (*inset*). *Each bar* represent the mean ± SD of four independent experiments $*p < 0.05$ versus control, $**p < 0.001$ vs control, and $\phi$ $p < 0.05$ versus NP without Tlx. ANOVA, Tukey

## Discussion

In this study, we investigated the influence of the physicochemical characteristics and probable oxidant properties of CIGS and CdS in relation to the induction of cytotoxicity in A549 cells. We used human lung epithelial cell line A549 to identify the potential cytotoxicity of CIGS and CdS NP because pulmonary epithelial cells would represent one of the first exposed tissues to NP released in the manufacture or disposal of PV devices. CIGS NP were highly cytotoxic to A549 cells in mass-based comparison to CdS; this finding has important implications in the synthesis, manufacture, and disposal of PV considering that CIGS is present in 30–40-fold with respect to CdS, in these devices. Although CIGS and CdS NP possess poor colloidal stability in culture media, according to the European Commission (2011) both materials are still in nano-size range, since the threshold limit established to define NP states that "50 % or more of the particles in the size range 1 nm–100 nm" and can be reduced in cases where potential risks to the environment and health are suspected.

Our study shows that CIGS, but not CdS NP, are reactive particles toward DTT, this behavior could be explained in part by its semiconductor nature. CIGS NP are designed to be used as absorber material in PV systems, because of its p-type (positive) semiconducting characteristics (Vidhya 2010); thus this material possesses an excess of holes or vacancies of electrons making it able to capture and mobilize electrons derived from sunlight photons. If we consider that DTT is a potent reducing agent that is partially ionized at physiological pH, it is probable that CIGS can remove electrons from the thiol groups in the DTT and then transfer them to the oxygen thus increasing the ROS in its microenvironment. On the other hand, CdS NP are

synthesized with the purpose to behave as a n-type semiconductor, in which its structure possesses an excess of electrons or negative carriers (Reyes and Velumani 2012). It is therefore likely that CdS NP are incapable of yielding the one-electron transfer from the DTT to the NP needed to initiate the oxidation reaction.

In addition, other explanation for these events is the oxidant reactivity based on the band gap energy of semiconductors (Burello and Worth 2011; George et al. 2011). This model describes how a semiconductor NP, like CIGS and CdS, can produce free radicals like $O_2^-$ and OH• by taking energy from cytophysiological reactions and mobilizing electrons from its own valence band (VB) (the highest energy levels in a solid that is fully occupied by electrons) to the conduction band (CB) (the lowest vacant energy level in which electrons move freely), leaving behind both holes in the conduction band that can be filled out by disruption of water molecules, and free electrons in the valence band that can be transferred to oxygen (Hoffmann et al. 1995). The energy needed to trigger the movement of free electrons from VB to CB is called band gap energy. Considering this, it is probable that CIGS NP are more reactive because they require less energy to move its electrons due to its low band gap energy of approximately 1.0 eV compared to 2.42 eV of CdS NP. This mechanism could also explain why CIGS produce higher amounts of $H_2O_2$ inside the cells as compared to CdS due to the generation of $O_2^-$ and its consequent conversion by the superoxide dismutase. Moreover, Zhang et al. (2012) have correlated the band gap values of several metal oxide NP to their ability to induce oxidative stress and inflammation in vitro and in vivo models. In contrast to the acellular approach, CdS induced a slight, but significant, amount of intracellular $H_2O_2$; the oxidative properties observed between acellular and cellular approaches, suggest the possibility that the observed biological response could be mediated mainly by the interaction between the NP with vital cell structures or organelles such as the mitochondria or lysosomes and not due to an intrinsic oxidative property of the particle, as reported for other NP such as cationic polystyrene, ZnO, $Fe_3O_4$, and $SiO_2$ (Xia et al. 2006; Unfried et al. 2007; Pal et al. 2011; Escamilla-Rivera et al. 2016).

Regardless of their different oxidant activities, both CIGS and CdS NP impair mitochondrial function almost to the same extent, which is reflected by the depolarization of the inner membrane of mitochondria. Several proteins inside mitochondria such as the ones that are part of the permeability transition pore (PTP) are sensitive to ROS; once they are oxidized they are recruited in order to form the PTP complex leading to influx of ions, loss of the $\Delta\psi m$, and mitochondrial swelling (Orrenius et al. 2007). It is well known that this organelle is a main source of ROS inside the cell, where approximately 1–2 % of oxygen consumed is converted to $O_2^-$ by the mitochondrial electron transport chain, a process susceptible to be uncoupled by xenobiotics (Kowaltowski et al. 2009). Based in our findings and TEM micrographs, it is possible to speculate that a small fraction of CIGS NP are able to interact directly with mitochondria (probably with complexes I and III) uncoupling redox reactions, inducing a loss of the $\Delta\psi m$, and leading to ROS overproduction. Impairment in mitochondria function has been found to be a key event in the toxicity mechanisms associated with several NP. For example, Teodoro et al. (2011) demonstrated that the interaction of isolated mitochondria with Ag NP led to an uncoupling effect of the oxidative phosphorylation. Moreover, Freyre-Fonseca et al. (2011) demonstrated that direct interaction of $TiO_2$ NP impairs lung mitochondria activity inducing loss of the $\Delta\psi m$ and an increment of intracellular ROS.

Moreover, induced cell death by apoptosis and mitochondrial damage from exposure to CIGS and CdS NP seemed to be dependent to the type of NP being more extensive in response to CIGS exposure. Apart from its role in ROS production, mitochondrial dysfunction could also promote apoptosis due to bioenergetics deficit since $\Delta\psi m$ also is required to perform oxidative phosphorylation to produce ATP. In this context, Tedja et al. (2011) demonstrated that A549 cells exhibit a decrement in mitochondrial activity and a depletion of cellular ATP after being exposed to $TiO_2$ NP. Furthermore, opening of PTP results in mitochondrial swelling, outer membrane rupture, and release of mitochondrial proteins like cytochrome *c*, a critical protein for caspase activation through mitochondrial pathway, and is also an important amplification step for death receptor ligand in apoptosis (Ott et al. 2007).

It is noteworthy that Trolox pretreatment protected A549 cells from the depolarization of mitochondria

and cell death induced by CIGS and CdS exposure. Trolox acts as an intracellular hydrogen supplier, which can be coupled to unpaired electrons present in free radicals. It has been proven that this antioxidant can prevent oxidation of mitochondrial lipids, (Izyumov et al. 2010), loss in MMP (Zorov et al. 2000), and reduce the induction of apoptosis originated through this pathway (Forrest et al. 1994). Therefore, is clear that only when the antioxidant defense is overwhelmed, NP-induced ROS can exert its deleterious effects through biomolecules oxidation and lead the cell to an oxidative stress status. In the present study, it is clearly demonstrated that ROS are the main intermediates in the mechanism of toxicity induced by CIGS and CdS NP in A549 cells. Although some differences can be found at the triggering mechanisms, the increment of intracellular ROS is in agreement with the toxicity of other type of NP like ZnO NP (Huang et al. 2010), $TiO_2$ (Ghiazza et al. 2014), $Fe_3O_4$ (Escamilla-Rivera et al. 2016), and Ag (Wang et al. 2014).

Since our work demonstrates the toxic potential of CIGS and CdS NP, and considering the important potential for an industrial scale development of PV modules, it is of relevant interest to investigate the long-term effects of exposure to these NP. CIGS due to its cytotoxicity to A549, could induce irreparable alveolar epithelial damage, possibly leading to pulmonary fibrosis. CdS NP were located principally in lamellar bodies that are the responsible for surfactant synthesis and could interfere with its functions, such as protein A surfactant production. Notwithstanding, we did not evaluate the persistence or potential dissolution of NP; this possibility cannot be excluded. The presence of CdS within acidic compartments could favor a dissolution process, and could act as a Cd source inside the cell, a mechanism of injury previously seen with quantum dots (Hardman 2006), and that should be addressed in future studies.

## Conclusions

In summary, CIGS, possibly due to its semiconductor properties, possess an intrinsic redox ability, which is related with a higher increase in intracellular ROS and the loss of mitochondrial function and ultrastructure. Altogether, CIGS-induced effects culminated in the induction of a severe cytotoxicity in A549 cells, whereas CdS NP induced an increment in ROS only after being up taken by A549 cells where they accumulate in lamellar bodies inducing moderate mitochondria impairment and leading to apoptosis. Antioxidant pretreatment confirms that the main pathway of toxicity of CIGS and CdS NP is the generation of intracellular ROS in A549 cells. The present study addresses the concern about the lack of toxicological information for semiconductor NP, and particularly for CIGS and CdS NP that are intended to improve PV panels. Therefore, the findings presented here would be a valuable resource on future risk assessment for a safer use of nanotechnology in the development of clean sources of renewable energy.

**Acknowledgements** This research project was supported partially by Project No. ICyT-DF 396/10.

## References

Bagnall DM, Boreland M (2008) Photovoltaic technologies. Energy Policy 36:4390–4396. doi:10.1016/j.enpol.2008.09.070

Burello E, Worth AP (2011) A theoretical framework for predicting the oxidative stress potential of oxide nanoparticles. Nanotoxicology 5:228–235. doi:10.3109/17435390.2010.502980

Cho AK, Sioutas C, Miguel AH, Kumagai Y, Schmitz DA, Singh M, Eiguren-Fernandez A, Froines JR (2005) Redox activity of airborne particulate matter at different sites in the Los Angeles Basin. Environ Res 99:40–47

De Vizcaya-Ruiz A, Gutiérrez-Castillo ME, Uribe-Ramirez M, Cebrián ME, Mugica-Alvarez V, Sepúlveda J, Rosas I, Salinas E, Garcia-Cuéllar C, Martínez F (2006) Characterization and in vitro biological effects of concentrated particulate matter from Mexico City. Atmos Environ 40:583–592. doi:10.1016/j.atmosenv.2005.12.073

Dhere NG (2007) Toward GW/year of CIGS production within the next decade. Sol Energy Mater Sol Cells 91:1376–1382. doi:10.1016/j.solmat.2007.04.003

Dreher KL (2004) Health and environmental impact of nanotechnology: toxicological assessment of manufactured nanoparticles. Toxicol Sci 77:3–5. doi:10.1093/toxsci/kfh041

Eisenberg DA, Yu M, Lam CW, Ogunseitan OA, Schoenung JM (2013) Comparative alternative materials assessment to screen toxicity hazards in the life cycle of CIGS thin film photovoltaics. J Hazard Mater 260:534–542. doi:10.1016/j.jhazmat.2013.06.007

Escamilla-Rivera V, Uribe-Ramírez M, González-Pozos S, Lozano O, Lucas S, De Vizcaya-Ruiz A (2016) Protein corona acts as a protective shield against $Fe_3O_4$-PEG inflammation and ROS-induced toxicity in human macrophages. Toxicol Lett 240:172–184. doi:10.1016/j.toxlet.2015.10.018

European Commission (2011) Commission Recommendation of 18 October 2011 on the definition of nanomaterial. Off J Eur Union 50:38–40

Forrest VJ, Kang YH, McClain DE, Robinson DH, Ramakrishnan N (1994) Oxidative stress-induced apoptosis prevented by Trolox. Free Radic Biol Med 16(6):675–684

Freyre-Fonseca V, Delgado-Buenrostro NL, Gutierrez-Cirlos EB, Calderon-Torres CM, Cabellos-Avelar T, Sanchez-Perez Y, Pinzon E, Torres I, Molina-Jijon E, Zazueta C, Pedraza-Chaverri J, Garcia-Cuellar CM, Chirino YI (2011) Titanium dioxide nanoparticles impair lung mitochondrial function. Toxicol Lett 202:111–119. doi:10.1016/j.toxlet.2011.01.025

Frick R, Müller-Edenborn B, Schlicker A, Rothen-Rutishauser B, Raemy DO, Günther D, Hattendorf B, Stark W, Beck-Schimmer B (2011) Comparison of manganese oxide nanoparticles and manganese sulfate with regard to oxidative stress, uptake and apoptosis in alveolar epithelial cells. Toxicol Lett 205:163–172. doi:10.1016/j.toxlet.2011.05.1037

Fthenakis V (2009) Sustainability of photovoltaics: the case for thin-film solar cells. Renew Sustain Energy Rev 13:2746–2750

Fthenakis V, Moskowitz PD (2000) Photovoltaics: environmental, health and safety issues and perspectives. Prog Photovoltaics Res Appl 8:27–38. doi:10.1002/(sici)1099-159x(200001/02)8:1<27:aid-pip296>3.0.co;2-8

George S, Pokhrel S, Ji Z, Henderson BL, Xia T, Li L, Zink JI, Nel AE, Mädler L (2011) Role of Fe doping in tuning the band gap of TiO2 for the photo-oxidation-induced cytotoxicity paradigm. J Am Chem Soc 133:11270–11278. doi:10.1021/ja202836s

Ghiazza M, Alloa E, Oliaro-Bosso S, Viola F, Livraghi S, Rembges D, Capomaccio R, Rossi F, Ponti J, Fenoglio I (2014) Inhibition of the ROS-mediated cytotoxicity and genotoxicity of nano-TiO2 toward human keratinocyte cells by iron doping. J Nanopart Res 16:1–17. doi:10.1007/s11051-014-2263-z

Hardman R (2006) A toxicologic review of quantum dots: toxicity depends on physicochemical and environmental factors. Environ Health Perspect 114:165–172

Hoffmann MR, Martin ST, Choi W, Bahnemann DW (1995) Environmental applications of semiconductor photocatalysis. Chem Rev 95:69–96. doi:10.1021/cr00033a004

Huang C, Aronstam R, Chen R, Huang W (2010) Oxidative stress, calcium homeostasis, and altered gene expression in human lung epithelial cells exposed to ZnO nanoparticles. Toxicol in vitro 24:45–55. doi:10.1016/j.tiv.2009.09.00

Izyumov DS, Domnina LV, Nepryakhina OK, Avetisyan AV, Golyshev SA, Ivanova OY, Korotetskaya MV, Lyamzaev KG, Pletjushkina OY, Popova EN, Chernyak BV (2010) Mitochondria as source of reactive oxygen species under oxidative stress. Study with novel mitochondria-targeted antioxidants — the "Skulachev-ion" derivatives. Biochem Moscow 75:123–129

Jackson P, Hariskos D, Lotter E, Paetel S, Wuerz R, Menner R, Wischmann W, Powalla M (2011) New world record efficiency for Cu(In, Ga)Se2 thin-film solar cells beyond 20%. Prog Photovoltaics Res Appl 19:894–897. doi:10.1002/pip.1078

Jiang J, Oberdörster G, Biswas P (2008) Characterization of size, surface charge, and agglomeration state of nanoparticle dispersions for toxicological studies. J Nanopart Res 11:77–89. doi:10.1007/s11051-008-9446-4

Kamp DW, Panduri VA, Weitzman S, Chandel N (2002) Asbestos-induced alveolar epithelial cell apoptosis: role of mitochondrial dysfunction caused by iron-derived free radicals. Mol Cell Biochem 234–235:153–160

Kowaltowski AJ, de Souza-Pinto NC, Castilho RF, Vercesi AE (2009) Mitochondria and reactive oxygen species. Free Radic Biol Med 47:333–343. doi:10.1016/j.freeradbiomed.2009.05.004

Kumagai Y, Koide S, Taguchi K, Endo A, Nakai Y, Yoshikawa T, Shimojo N (2002) Oxidation of proximal protein sulfhydryls by phenanthraquinone, a component of diesel exhaust particles. Chem Res Toxicol 15:483–489. doi:10.1021/tx0100993

Liu C-J, Burghaus U, Besenbacher F, Wang ZL (2010) Preparation and characterization of nanomaterials for sustainable energy production. ACS Nano 4:5517–5526. doi:10.1021/nn102420c

Martindale JL, Holbrook NJ (2002) Cellular response to oxidative stress: signaling for suicide and survival. J Cell Physiol 192:1–15

Maynard AD (2007) Nanotechnology: the next big thing, or much ado about nothing? Ann Occup Hyg 51:1–12. doi:10.1093/annhyg/mel071

Mosmann T (1983) Rapid colorimetric assay for cellular growth and survival: application to proliferation and cytotoxicity assays. J Immunol Methods 65:55–63. doi:10.1016/0022-1759(83)90303-4

Nel A, Xia T, Mädler L, Li N (2006) Toxic potential of materials at the nanolevel. Science 311:622–627. doi:10.1126/science.1114397

Oberdörster G (2010) Safety assessment for nanotechnology and nanomedicine: concepts of nanotoxicology. J Intern Med 267:89–105. doi:10.1111/j.1365-2796.2009.02187.x

Orrenius S, Gogvadze V, Zhivotovsky B (2007) Mitochondrial oxidative stress: implications for cell death. Annu Rev Pharmacol Toxicol 47:143–183. doi:10.1146/annurev.pharmtox.47.120505.105122

Ott M, Gogvadze V, Orrenius S, Zhivotovsky B (2007) Mitochondria, oxidative stress and cell death. Apoptosis 12:913–922

Pal AK, Bello D, Budhlall B, Rogers E, Milton DK (2011) Screening for oxidative stress elicited by engineered nanomaterials: evaluation of acellular DCFH assay. Dose-Response 1:1–23. doi:10.2203/dose-response.10-036.Pal

Reinhard P, Buecheler S, Tiwari AN (2013) Technological status of Cu(In, Ga)(Se, S)2-based photovoltaics. Sol Energy Mater Sol Cells 119:287–290. doi:10.1016/j.solmat.2013.08.030

Reyes P, Velumani S (2012) Structural and optical characterization of mechanochemically synthesized copper doped CdS nanopowders. Mater Sci Eng B-Adv Funct Solid-State Mater 177:1452–1459. doi:10.1016/j.mseb.2012.03.002

Sauvain J-J, Deslarzes S, Riediker M (2008) Nanoparticle reactivity toward dithiothreitol. Nanotoxicology 2:121–129

Tedja R, Marquis C, Lim M, Amal R (2011) Biological impacts of TiO2 on human lung cell lines A549 and H1299: particle

size distribution effects. J Nanopart Res 13:3801–3813. doi:10.1007/s11051-011-0302-6

Teodoro JS, Simoes AM, Duarte FV, Rolo AP, Murdoch RC, Hussain SM, Palmeira CM (2011) Assessment of the toxicity of silver nanoparticles in vitro: a mitochondrial perspective. Toxicol In Vitro 25:664–670. doi:10.1016/j.tiv.2011.01.004

Unfried K, Albrecht C, Klotz LO, Von Mikecz A, Grether-Beck S, Schins RPF (2007) Cellular responses to nanoparticles: target structures and mechanisms. Nanotoxicology 1:52–71

Valko M, Leibfritz D, Moncol J, Cronin MTD, Mazur M, Telser J (2007) Free radicals and antioxidants in normal physiological functions and human disease. Int J Biochem Cell Biol 39:44–84

Vidhya B, Velumani S, Arenas-Alatorre JA, Morales-Acevedo A, Asomoza R, Chavez-Carvayar JA (2010). Structural studies of mechano-chemically synthesized $CuIn_{1-x}Ga_xSe_2$ nanoparticles. Mater Sci Eng B 174: 216–221. doi:10.1016/j.mseb.2010.03.014

Wang L, Pal AK, Isaacs JA, Bello D, Carrier RL (2014) Nanomaterial induction of oxidative stress in lung epithelial cells and macrophages. J Nanopart Res 16:1–14. doi:10.1007/s11051-014-2591-z

Xia T, Kovochich M, Brant J, Hotze M, Sempf J, Oberley T, Sioutas C, Yeh J, Wiesner M, Nel A (2006) Comparison of the abilities of ambient and manufactured nanoparticles to induce cellular toxicity according to an oxidative stress paradigm. Nano Lett 6:1794–1807. doi:10.1021/nl061025k

Xia T, Kovochich M, Liong M, Ma dler L, Gilbert B, Shi H, Yeh JI, Zink JI, Nel A (2008) Comparison of the mechanism of toxicity of zinc oxide and cerium oxide nanoparticles based on dissolution and oxidative stress properties. ACS Nano 2:2121–2134 doi:10.1021/nn800511k

Zhang H, Ji Z, Xia T, Meng H, Low-Kam C, Liu R, Pokhrel S, Lin S, Wang X, Liao Y-P, Wang M, Li L, Rallo R, Damoiseaux R, Telesca D, Mädler L, Cohen Y, Zink JI, Nel A (2012) Use of metal oxide nanoparticle band gap to develop a predictive paradigm for oxidative stress and acute pulmonary inflammation. ACS Nano 6:4349–4368. doi:10.1021/nn3010087

Zorov DB, Filburn CR, Klotz L-O, Zweier JL, Sollott SJ (2000) Reactive oxygen species (ROS-induced) ROS release: a new phenomenon accompanying induction of the mitochondrial permeability transition in cardiac myocytes. J Exp Med 192(7):1001–1014